

---

# ASTEC participation in the International Standard Problem on KAEVER

P. Spitz<sup>\*</sup>, J. P. Van Dorsselaere<sup>\*</sup>, B. Schwinges<sup>\*\*</sup>, S. Schwarz<sup>\*\*</sup>

*<sup>\*</sup>Institut de protection et de sûreté nucléaire, Département de Recherches en Sécurité,  
CEA Cadarache - 13108 St Paul lez Durance - France*

*<sup>\*\*</sup>Gesellschaft für Anlagen und Reaktorsicherheit mbH,  
Schwertnergasse 1 - 50667 Cologne - Germany*

---

**Abstract:** The objectives of the International Standard Problem N°44 was aerosol depletion behaviour under severe accident conditions in a LWR containment examined in the KAEVER test facility of Battelle (Germany). Nine organisations participated with 5 different codes in the ISP44, including a joint participation of GRS and IPSN with the integral code ASTEC (and in particular the CPA module) they have commonly developed. Five tests were selected from the KAEVER test matrix: K123, K148, K186 and K188 as open standard problems and the three-component test K187 as blind standard problem. All these tests were performed in supersaturated conditions and with slight fog formation, which are the most ambitious conditions for the coupled problem of thermal hydraulics and aerosol processes. The comparison between calculation and test showed a good agreement for all the tests with respect to the thermal-hydraulic conditions in the vessel, i.e. total pressure, atmosphere temperature, sump water and nitrogen mass, etc.... As for aerosol depletion, the ASTEC results were in a good overall agreement with the measured data. The code in particular predicted well the fast depletion of the hygroscopic and mixed aerosols and the slow depletion of insoluble silver aerosol. The important effects of bulk condensation, solubility and the Kelvin effect on the aerosol depletion were well predicted. However the code overestimation of steam condensation on hygroscopic aerosols in supersaturated conditions indicates that some slight improvements of the appropriate ASTEC models are needed in the future. In the final ISP44 workshop, the deviations of the ASTEC results with respect to the experiments were considered to be small compared to those of most other codes.

## 1. INTRODUCTION

The French-German integral code ASTEC (**A**ccident **S**ource **T**erm **E**valuation **C**ode) is developed commonly by IPSN and GRS with the aim to get a fast-running code for the simulation of the complete sequences of severe accidents in LWR (Light Water Reactors) from the initiating event up to the possible fission product release to the environment. The code can be applied to accident sequence studies, probabilistic safety assessments, investigations on accident management procedures and support to tests. For a basic validation, a matrix containing a minimum set of necessary tests was defined. For further validation and comparative assessment with other codes and users, IPSN and GRS participated together with the ASTEC code in the blind International Standard Problem 44 (ISP44). The detailed comparison of the data permits conclusions for the predictive capability

of computer simulations of postulated accidents and contributes to the further development and improvement of the code.

During an unmitigated severe LWR accident, radioactive fission and activation products are being released into the containment and to a great extent adsorbed on aerosols, while the containment building serves as a final barrier to the environment. Thus, a detailed knowledge of fission products and aerosol behaviour and a relevant analytical predictive capability are of great importance for evaluation of possible release to the environment, e.g. by venting or leakage.

Following a suggestion of the Federal Republic of Germany, the OECD-CSNI proposed tests from the KAEVER test series [1], performed at Battelle, Eschborn, as ISP44 to its member countries. The test and the execution of the ISP were sponsored by the German Federal Ministry of Education and Research and by the German Federal Ministry of Economics and Technology, respectively. The general objective was to analyse the behaviour (e.g. bulk condensation and settlement) of aerosols in a containment atmosphere with well-defined thermal-hydraulic boundary conditions. The ISP was conducted as a "blind" standard problem, e.g. besides initial and boundary conditions, the relevant test results of test K187 had been locked and not delivered to the participants in the ISP prior to performing the calculation. In addition, results of four other KAEVER similar tests K123, K148, K186, K188 were available to the participants for "open" calculations.

## 2. DESCRIPTION OF TESTS

The KAEVER (**K**ernschmelz-**A**erosol-**V**ersuche) test facility was located at the Frankfurt site of Battelle, Germany. The test matrix of the KAEVER project comprised 32 tests that were carried out in this facility between 1991 and 1997. Objectives of these tests were to study the aerosol depletion in a medium-sized model of LWR containment and to establish a validation basis for code model development.

Thermal-hydraulic conditions, mainly humidity and degree of supersaturation, as well as the composition of the aerosols (different individual components or mixtures of several components) were varied in the tests. The KAEVER facility and the tests are described in detail in [1].

### 2.1. Description of Test Facility

The test containment of the KAEVER facility consisted of a cylinder with even front walls, rectangular door openings and sliding doors positioned outside (see Figures 1 and 2). The cylindrical part was 2500 mm long with an internal diameter of 2090 mm and a wall thickness of 25 mm. The door openings were 800 mm wide, 1900 mm high and had a wall thickness of 40 mm. The volume of the test containment was 10.595 m<sup>3</sup>. The cylinder and the doors were heated and insulated whereas the front walls were insulated only. The not insulated door opening mechanisms on the vessel outside acted like cooling fins and contributed to vessel heat losses.

The aerosols were generated in an induction furnace, a water-cooled steel pressure vessel containing a crucible with the aerosol material. Heating of the crucible was possible by either a high-frequency generator for high volatile aerosols, i.e. CsI and CsOH, or a static medium-frequency converter for low volatile aerosols, i.e. Ag. The generated aerosols were

transported by nitrogen through a heated and insulated line to the test containment and injected upwards, 30 cm below the upper wall, in the centre of the cylinder.

Steam coming from a steam generator was used to heat up the test containment and to adjust quasi-stationary thermal-hydraulic conditions during the aerosol injection and depletion phase. The steam was injected 15 cm above the lower wall in the centre of the cylinder.

Numerous sensors measured the thermal-hydraulic conditions in the test containment, i.e. pressure, humidity and temperatures of atmosphere, sump and structures. The sophisticated aerosol measuring technology comprised a filter exchange bench, a mobility analyser and condensation nuclear counter, an aerodynamic particle sizer, a transmission monitoring system, a spectral extinction photometer and impactors.

## **2.2 Conduct of Tests**

Each test consisted in principle of two phases, the preconditioning phase (Phase I) and the aerosol phase (Phase II). The objective of Phase I was to obtain quasi-stationary conditions in the test containment. Therefore, the vessel was flushed with steam and the walls were electrically heated to reach elevated temperatures. The data acquisition system was not completely operating during this phase. At the end of this phase, sump water was withdrawn from the vessel. During Phase II, the aerosols were injected and the aerosol depletion measured. The atmosphere was slightly supersaturated resulting in a slight fog formation and in steam condensation on the aerosol particles in all five tests selected for the ISP44.

The general characteristics were:

### **Open Tests:**

- Test K123: soluble CsI aerosols were injected,
- Test K148: insoluble aerosols of Ag were injected. At the beginning of Phase II the sump contained already some water and the atmosphere some nitrogen from the clearing gas.
- Test K186: mixed aerosols of Ag and CsOH were injected,
- Test K188: soluble CsOH aerosols were injected.

### **Blind Test:**

- Test K187: mixed aerosols of Ag, CsOH and CsI were injected.

## **3. CODE DESCRIPTION**

The French-German integral code ASTEC (Accident Source Term Evaluation Code) [3] is being developed by IPSN (Institut de Protection et de Sûreté Nucléaire), France, and GRS (Gesellschaft für Anlagen- und Reaktorsicherheit), Germany, since 1994. The first version (ASTEC V0), already released to several European organisations, has been based on the best models of the French integral code ESCADRE and on the German containment codes RALOC for thermal-hydraulics and FIPOC for aerosol behaviour. The main models in the latter code [5] were based on the MAEROS code, developed by Sandia National Laboratories, USA.

Only the ASTEC module CPA was activated in the calculation of the KAEVER tests to

describe thermal-hydraulics and aerosol behaviour in the containment.

### 3.1 CPA Module Description

A comprehensive overview about module CPA is given in the user guidelines manual [4] and the aerosol models are described in detail in [5]. Therefore, only an overview about the most important models with respect to the calculation of the KAEVER tests will be given here.

The module CPA is a “lumped-parameter” or “multi-zone” code. It consists of a thermal-hydraulic part (CPA-THY) and an aerosol and fission product part (CPA-AFP).

#### 3.1.1 CPA-THY

In this exercise only a small part of the thermal-hydraulic capabilities was used:

- pressure and temperature build up and history,
- energy distribution, heat transfer and heat conduction in structures.

For the KAEVER aerosol simulations the most important variables are the bulk condensation rate and the atmospheric humidity.

#### 3.1.2 CPA-AFP

The aerosol model describes the behaviour of a homogeneously mixed polydispersed aerosol system inside a control volume. The system may be composed of up to 8 chemically different aerosol components. Agglomeration, condensation, deposition and existing aerosol sources (injections) and sinks (aerosol discharges) are calculated. The particle size range is discretised by a maximum of 20 particle size categories. Each size category may be differently composed of the various chemical components. However, within each category a homogenisation will be performed so that all particles of one given category will have the same component composition.

#### Agglomeration processes

The process referred to as agglomeration or coagulation describes what happens when two or more particles collide, stick to each other and form a larger particle. The agglomeration rate rises quadratically with the particle number concentration. In LWR containment, considerable agglomeration rates can be expected from about 1 g/m<sup>3</sup> aerosol concentration. Four different aerosol processes are modelled (here the two first processes are dominant):

- Brownian agglomeration,
- gravitation agglomeration,
- turbulent shear agglomeration,
- turbulent inertial agglomeration.

Brownian agglomeration takes place through the Brownian movement of aerosol particles in the gas. It is the dominating effect in containment. It is proportional to the agglomeration factor  $\gamma$  and reverse proportional to the shape factor  $\chi$ . With these factors, the deviation of the particles from the spherical form is taken into account. For spherical particles  $\gamma = \chi = 1$ .

The gravitational agglomeration takes into account the collision of large, faster falling particles with smaller and thus slower ones. The collision efficiency  $\varepsilon$  for the gravitational agglomeration indicates the probability with which particles that collide will actually stick to each other. Different relations for  $\varepsilon$  are available in CPA-AFP: Fuchs relation, Pruppacher-Klett one and the original MAEROS one. The agglomeration rate increases with growing

collision efficiency and increasing agglomeration factor. It decreases with increasing shape factor.

### **Deposition processes**

The aerosol model takes the following deposition processes into account:

- sedimentation,
- diffusive deposition,
- thermophoresis,
- diffusiophoresis.

Like the agglomeration coefficients, the deposition coefficients are not calculated anew for each time interval but are determined from a table of coefficients drawn up at the start of the calculations by interpolation in line with the overall pressure and the temperature. Sedimentation is the deposition of particles on floor surfaces by gravity. As the sedimentation process in a well-mixed volume takes place in a thin boundary layer along the surface, all horizontal surfaces serve as sedimentation surfaces. In LWR containment, sedimentation is generally the most effective deposition process.

Deposition through diffusion takes place as Brownian movement in the concentration gradient on the surface. It is mainly relevant for small particles. The user must provide the boundary layer thickness.

Thermal-hydraulic deposition of aerosol particles takes place in the temperature gradient of a boundary layer on a cold wall. In LWR containment it only plays a subordinate role since there are no great temperature differences between the dry atmosphere and the wall. The aerosol model uses an empiric value of 3 mm for the thermophoretic boundary layer thickness. Diffusiophoretic deposition takes place through steam condensation on a cold wall caused by the aerodynamic Stefan flow.

### **Condensation method MGA**

Condensation on the particles is calculated with the moving-grid-method MGA. It reduces calculation times and the numeric diffusion compared to the fixed-grid method. The moving-grid method to calculate condensation on particles was developed by F. Gelbard (Sandia National Laboratories, USA). During the calculation, the grid of the particle size categories is apparently moved. In the case of the conventional fixed-grid method, growing particles are passing through the grid. The thermal-hydraulic model (CPA-THY) and the aerosol models (CPA-AFP) have their own time integration in the program system and are closely coupled to each other. During the condensation interval, the thermal-hydraulic boundary conditions remain constant. They are only updated before the next interval. However, MGA is internally performing a simplified thermal-hydraulic calculation. In the aerosol interval that follows, the wet aerosol is treated like a dry one. Agglomeration and deposition of the droplets are calculated as if they were solid particles, i.e. the amount of airborne water and its distribution to the solid particles is not altered. In the MGA method, the particle growth and particle shrinking rate are given by the Mason equation.

With the surface tension, the influence of the Kelvin effect on the particle growth is taken into account. The Kelvin effect depends strongly on the particle size. The hygroscopic effect is described in the equation by the chemical activity of the solution, which is determined by the Vant'Hoff factor. It corresponds to the number of ions into which a molecule of the salt dissociates in an ideal solution (e.g.  $a_w = 2$  for NaOH). For insoluble substances,  $a_w = 0$ . In MGA the assumption is that there is always an ideal solution present in which the chemical activity decreases at an increasing molar proportion of the water in a droplet.



## 3.2 Computational Model

### Code version

The calculations for ISP44 were performed with ASTEC Version 0.3 from October 2000. No modifications were introduced into this version. Only the module CPA was activated in the calculations.

### Nodalisation

The test containment was modelled by one non-equilibrium zone with a volume of 10.595 m<sup>3</sup>. The non-equilibrium model, applied in a zone, handles the behaviour of different components (water, steam, and incondensable gases) : the sump temperature can be different from gas temperature (the temperature of liquid water present in the atmosphere as fog is equal to the gas one). The sump surface, i.e. the interface area between the liquid and the gaseous zone part was 3 m<sup>2</sup>. Note that the variation of sump surface vs. sump depth due to the vessel cylindrical form could not be accounted for. The environment surrounding the test containment was modelled by one equilibrium zone.

An atmospheric junction simulating small mass losses through the leaky door opening mechanism connected both zones. The cross section and pressure loss coefficients of the junction have been chosen according to the values proposed in the Specification Report [2]. The 3 components (water, steam and air) were represented in the zones. Component air was defined with the properties of nitrogen and simulated the nitrogen in the test. The aerosol module of CPA [4] requires the definition of either component air or a mixture of the components nitrogen and oxygen. The oxygen in the vessel was removed in the tests already during the initial flushing of the vessel with steam in the preparatory phase.

The walls of the test vessel have been modelled by 9 plate-type structures. The meshing of the material layers of the structures was equidistant. The steel layer has been subdivided in 2 layers, an inner layer of 2 mm with 2 meshes in contact with the containment atmosphere and a second layer with 5 meshes for the remaining thickness. This subdivision became necessary because, in the calculation of the condensation heat transfer, the temperature of the first inner mesh was used instead of the surface temperature, thus avoiding the iteration of the surface temperature. Therefore, it is advised to use thin meshes for the material layer in contact with the atmosphere when using that option. A thermal insulation layer (10 meshes) and an additional steel layer (2 meshes) 2 mm thick covered the insulated wall parts.

As proposed in the specification report, the cooling fin effect of the door opening mechanism was modelled by an artificial structure (structure N°10) in contact with the vessel atmosphere.

An additional structure (structure N°11) was modelled to simulate the room walls surrounding the test facility. This structure exchanged with the environment zone by convective heat transfer and with the outer surfaces of the vessel wall structures by radiative heat transfer.

The heat transfer modes on the internal side of the structures in contact with the vessel atmosphere were free and forced convection, condensation and wall-gas-radiation. The structures with orientation type 'floor' (structures 4, 5 and 6) were in contact with sump in the non-equilibrium zone. The heat transfer modes were limited here to free and forced convection. The heat transfer modes on the outer side of the structures in contact with the environment zone were free and forced convection, condensation and radiation from wall to wall.

**Table 1:** Main Characteristics of Vessel Wall Structures

Structure	Area (m <sup>2</sup> )	Orientation	Structure	Area (m <sup>2</sup> )	Orientation
1	4.07	Ceiling	7	11.73	side wall
2	0.235	Ceiling	8	4.685	side wall
3	1.372	Ceiling	9	1.85	side wall
4	4.07	Floor	10	2.35	side wall
5	0.235	Floor	11	1000	side wall
6	1.372	Floor			

The thermal properties of the structure materials were set as proposed in the specification report.

**Table 2:** Thermal Properties of Structure Materials

Material	Conductivity (W/m/K)	Heat capacity (J/kg/K)	Density (kg/m <sup>3</sup> )
Steel	45	480	7850
Insulation	0.091	840	110

### Aerosol Model Parameters

The aerosol deposition areas in the vessel were set according to the specifications [2], i.e. 7 m<sup>2</sup> for floor and ceiling and 17.6 m<sup>2</sup> for side walls. The injected aerosols were simulated by one to three components, accordingly to the test number, and the water condensing on the aerosols by an additional component. The components were assumed to be homogeneously mixed. They were divided into 20 size classes between 0.01  $\mu\text{m}$  and 100  $\mu\text{m}$ . The density of the aerosols was assumed to be 1100 kg/m<sup>3</sup> for tests where water condensed on the aerosols dominated the average particle density. The solubility (Van't Hoff factor) was set according to the specifications to 2 for component CsOH, to 1.7 for component CsI and to 0 for component Ag. Shape factor and agglomeration factor were set to 1. In the three-component test K187, it was assumed that the silver particles are well mixed with the other components because of the simultaneous injection of the three components and the comparable size distribution. The Kelvin effect could be neglected in all tests with soluble aerosols (such as K187) because of the high solubility of the particles. It was only regarded in test K148 with silver aerosols.

### Initial and Boundary Conditions

Since the experimental conditions of Phase I (initial and boundary conditions given in the specification report) were not sufficiently known, this Phase I was simulated in a way to reach measured initial conditions of Phase II.

A transient of 100000 s was assumed for Phase I. The initial conditions were a pressure of 1.9 bar, a temperature of 104 °C and a humidity of 100 % for the non-equilibrium zone modelling the vessel, and a pressure of 1 bar, a temperature of 20 °C and a humidity of 80 % for the equilibrium zone modelling the environment.

The boundary conditions during Phase I were as follows:

- slightly superheated steam was injected at a rate of initially 7 g/s and later on 3 g/s. The total power brought to the heated structures 1, 4 and 7 was distributed to the structures according to their surface ratio.
- air was withdrawn from the vessel by a negative nitrogen source at the beginning of Phase I.
- condensed water in the vessel was withdrawn from the sump by a negative water source in tests at the end of Phase I (except in test K148).

The boundary conditions specified by the Specification Report for Phase II were used for the injection of steam, as well as for the removal of nitrogen due to probe taking. The heating of the walls was turned off in all tests during Phase II, except for test K123. The sedimentation coupons in the vessel indicated that about 50 % of the aerosols generated in the crucible were trapped in the line leading to the vessel. Furthermore, very large particles present in the injected aerosols deposited rapidly and did not contribute to the measured aerosol concentrations. Time span and shape of aerosol injection were estimated from pyrometer and photometer measurements. Since the resulting aerosol injection rates given in the specification report still contained large uncertainties, it was recommended to adjust them such that the calculated aerosol concentrations met the first measured concentrations after the end of aerosol injection.

Besides, the size of the structure N°10 simulating the cooling fin effect of the door opening mechanisms was found to be between 2.35 and 2.5 m<sup>2</sup> by the ASTEC calculations for the tests without wall heating and 3.65 m<sup>2</sup> for the test with wall heating. These values allowed to obtain a good agreement between calculated and measured atmosphere temperatures.

**Table 3:** Modifications of data with respect to the Specification Report

Test	K123	K148	K186	K188	K187
Adjusted Surface of structure N°10 (m <sup>2</sup> )	3.65	2.35	2.5	2.35	2.35
Factor of modification of aerosol injection rate	0.98	0.5	0.7	1.4	0.33

The following table summarizes the important aerosol parameters for the blind case.

**Table 4:** Aerosol Parameters for K187 case

Test	Injected Mass (g)	Number Median Diameter (µm)	Standard Deviation
K187	11.4 (total) 1.1 (Ag), 4.2 (CsOH), 6.1 (Csl)	0.315	1.3

## 4. CALCULATION/TEST COMPARISONS

### Comparison of calculated concentrations of the injected aerosol material (Figures 3 to 7)

For the hygroscopic and mixed aerosols, the concentration of the injected materials decreased rapidly during the depletion phase as it is expected for wet conditions in the vessel, due to water condensation on the aerosols. Sedimentation is the main aerosol removal mechanism acting in the vessel. Particle growth by condensation on aerosols is then an active and favourable factor for gravity deposition. The smallest aerosol particles are less dependent on this phenomenon due to the Kelvin effect that prevents condensation on them. The comparison code/measurements is satisfactory, but with an overestimation of the depletion velocity.

Note that CPA could not reproduce the constant final concentration in the K123 test. This discrepancy is assumed to be linked to the measurement uncertainties. Let us recall that it is usually very difficult to measure on filters very small aerosol concentrations. In a series of experimental measurements, they are usually considered as the ones carrying the biggest uncertainty.

For insoluble silver (K148), the slower depletion than in the other tests (only somewhat faster than the aerosol depletion in a superheated atmosphere) was reproduced too, but with an underestimation with respect to the measured depletion velocity. As shown by the ASTEC results, the Kelvin effect is the main reason for this slow depletion. For example at 1000 s after the end of aerosol injection, it prevents condensation on particles smaller than 1.6  $\mu\text{m}$ , resulting in a slow settling of these particles. This effect works only on insoluble material. On hygroscopic material however the condensate is distributed uniformly on all particles.

### Further aerosol results

The calculated concentration of airborne water increased during the aerosol injection phase, and reached high concentrations caused by condensation on the injected particles. Then, during the depletion phase, the concentration decreased initially fast and remained then nearly constant because the bulk condensation rate was approximately constant. The airborne water concentration might be overestimated in the numerical simulations (see the following chapter).

Aerosol deposition was dominated by sedimentation to floors and water pool covering the floor. The deposits on walls were drained to the pool both in the experiment and in the calculation. It is not known what the deposition was in reality in the vessel: no comparison is thus possible.

The calculated mass median diameter of the wet aerosol (injected particles plus airborne water) increased during the aerosol injection phase and was then constant during the aerosol depletion phase. Since the mass median diameter for the dry aerosol, given for comparison in the specifications, is not part of the output of the CPA-AFP module, no comparison is thus possible.

### Thermalhydraulics

The thermal-hydraulic conditions in the vessel like total pressure, atmosphere temperature, sump water and nitrogen mass were correctly reproduced.

But in general, the sump temperature could not be reproduced correctly: the calculated sump temperature was closer to the atmosphere temperature than the measured sump temperature (the relative discrepancy was always lower than 10 to 15%). The origin of this

discrepancy is the modelling difficulty to simulate the real geometry of the facility: the exchange surfaces between sump and atmosphere and between sump and walls varied in the test with the sump water mass due to the cylindrical geometry of the vessel, whereas constant areas had to be assumed in the calculation.

### **Specific case of Blind test K187**

The calculated concentrations of the 3 aerosol components met the measured concentrations at the end of the aerosol injection phase. The concentration of the aerosol mixture decreased with about a factor of 100/ hour as shown on Figure 7.

The calculated concentration of the wet aerosols, consisting mostly of airborne water, increased during the aerosol injection phase to concentrations about  $33 \text{ g/m}^3$ , then decreased initially fast during the depletion phase and remained then nearly constant at about  $13 \text{ g/m}^3$ .

The calculated mass median diameter of the wet aerosol increased during the aerosol injection phase and was then around  $7 \mu\text{m}$  during the aerosol depletion phase. An initial mass median diameter of  $0.52 \mu\text{m}$  was specified for all three aerosol components. The extinction photometer indicated a mass median diameter of  $1.6 \mu\text{m}$  at the beginning of the depletion phase.

For aerosol deposition, in the calculation altogether 11.4 g were injected into the vessel, 9.6 g of it deposited on the floor, 1.5 g on the side walls, 0.1 g on the ceiling and 0.2 g evacuated through the leak to the environment.

## 5. MAIN OUTCOMES ON THE MODELS

The thermal-hydraulics was correctly reproduced by the code, except for sump temperature as explained in chapter 4.

Under slight fog formation, the code predicted well:

- the fast depletion of the hygroscopic and mixed aerosols in tests K123, K186, K187 and K188,
- the slow depletion measured for insoluble silver in test K148.

The important effects of bulk condensation, solubility and Kelvin effect on the aerosol depletion were well treated in the ASTEC code. The feedback of the hygroscopic water uptake by the aerosols on the thermalhydraulic conditions was taken into account in the calculations. Steam condenses on the aerosol particles due to supersaturated conditions resulting in fog formation and due to the hygroscopic effect. This is taken into account by the Mason equation. For the tests with hygroscopic aerosols, the calculated concentrations of the injected aerosol material indicated a slightly faster decrease than in the measurement. This indicates that the condensation on the aerosol particles might be overestimated for the conditions in the KAEVER tests. Besides, the dynamic calculation of the Kelvin effect in MGA is numerically not enough stable: for instance, the code stops if the fog formation rate becomes too low ( $< 0.02 \text{ g/m}^3/\text{s}$ ) or if the mean aerosol density is set too low ( $< 4000 \text{ kg/m}^3$ ). Some slight improvements of the models of steam condensation on hygroscopic aerosols should be performed in the future CPA versions.

In case of K187 the code assumption that the three materials have formed agglomerates is in good agreement with the test observations.

Besides, for the test K148 with pure insoluble silver, the measured dry aerosol concentrations indicated a lower decrease of the aerosol concentration than in the calculation. This discrepancy is probably dependent on the initial choice of apparent silver density in the calculation. The Kelvin effect hindered condensation of water on the smallest silver aerosols. Under weak fog formation the simulation of the Kelvin effect to calculate the behaviour of pure insoluble material is very important: this was well treated by ASTEC.

## 6. CONCLUSION

IPSN and GRS contributed jointly with the integral code ASTEC (version 0.3, module CPA) to the ISP44 on KAEVER tests (Battelle, Germany) involving aerosol depletion behaviour in severe accident conditions in LWR containment. Five tests were selected for the ISP44: K123, K148, K186 and K188 as Open Standard Problems and the three-aerosol component test K187 as the Blind Standard Problem. All these tests were performed in supersaturated conditions and with slight fog formation, which are the most ambitious conditions for the coupled problem of thermal hydraulics and aerosol processes. The conditions covered depletion of various types of aerosols, including insoluble silver aerosols as well as multi-component aerosols consisting of hygroscopic caesium hydroxide, caesium iodide and insoluble silver.

As for thermal-hydraulic conditions in the vessel, the comparisons between calculations and tests showed good agreement for all tests, except for sump temperature because of the difficulty of representing the real cylindrical geometry of the sump.

As for aerosol depletion, the ASTEC results showed a good overall agreement with the measured data. The code predicted in particular correctly the fast depletion of the hygroscopic and mixed aerosols as well as the slower depletion of insoluble silver aerosol. The important effects of bulk condensation, solubility and the Kelvin effect on aerosol depletion were well treated in the ASTEC code. However, the code overestimation of steam condensation on hygroscopic aerosols in supersaturated conditions indicates that some slight improvements of the appropriate models are needed in the future.

Nine organisations participated with 5 different codes in the ISP44. In the final workshop, the deviations of the ASTEC results with respect to the experiments were considered to be small compared to those of most other codes.

## REFERENCES

1. G. Poss, D. Weber, "Versuche zum Verhalten von Kernschmelzaerosolen im LWR-Containment - KAEVER", Battelle Abschlußbericht, BF-R-67863, Mai 1997.
2. M. Firnhaber, K. Fischer, B. Fritsche, "Specification of the International Standard Problem ISP N° 44: KAEVER - Tests on the Behaviour of Core-melt Aerosols in a LWR Containment", GRS mbH, January 2000.
3. H.J. Allelein, J. Bestele, K. Neu, F. Jacq, M. Kissane, W. Plumecocq, J.P. Van Dorsselaere, "Severe accident code ASTEC development and validation", EUROSAFE, Paris, November 1999.
4. J. Bestele, W. Klein-Heßling, "ASTEC V0 - CPA-module Containment Thermalhydraulics and Aerosol- and Fission Product Behaviour - User Guidelines", ASTEC-V0/DOC/00-14, GRS mbH, September 2000.
5. G. Weber, "Description of the Aerosol Models in FIPLOC 3.1, COCOSYS V1.0 and CPA in ASTEC V0", GRS-A-2700, GRS mbH, March 1999.

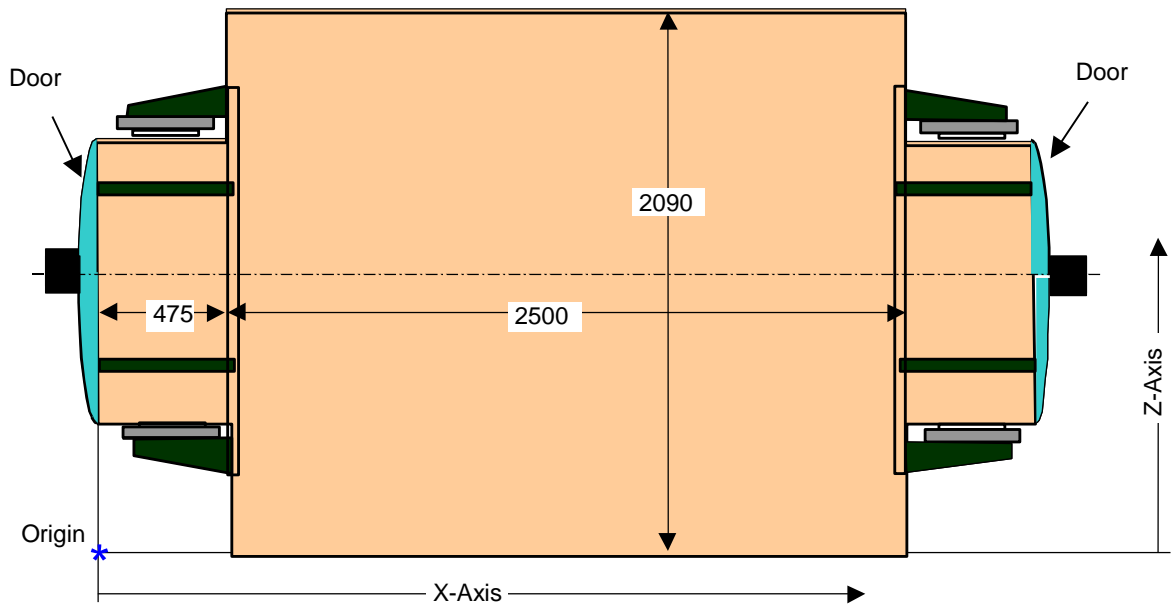


Figure 1: Top view of vessel

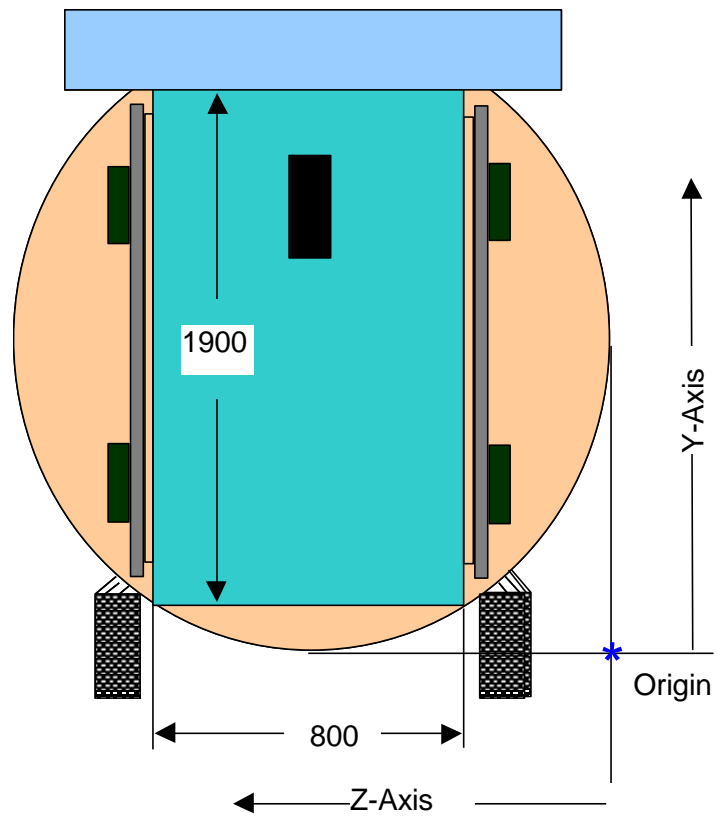


Figure 2: Front view of vessel

### K123 Total Dry Concentration (g/cm<sup>3</sup>)

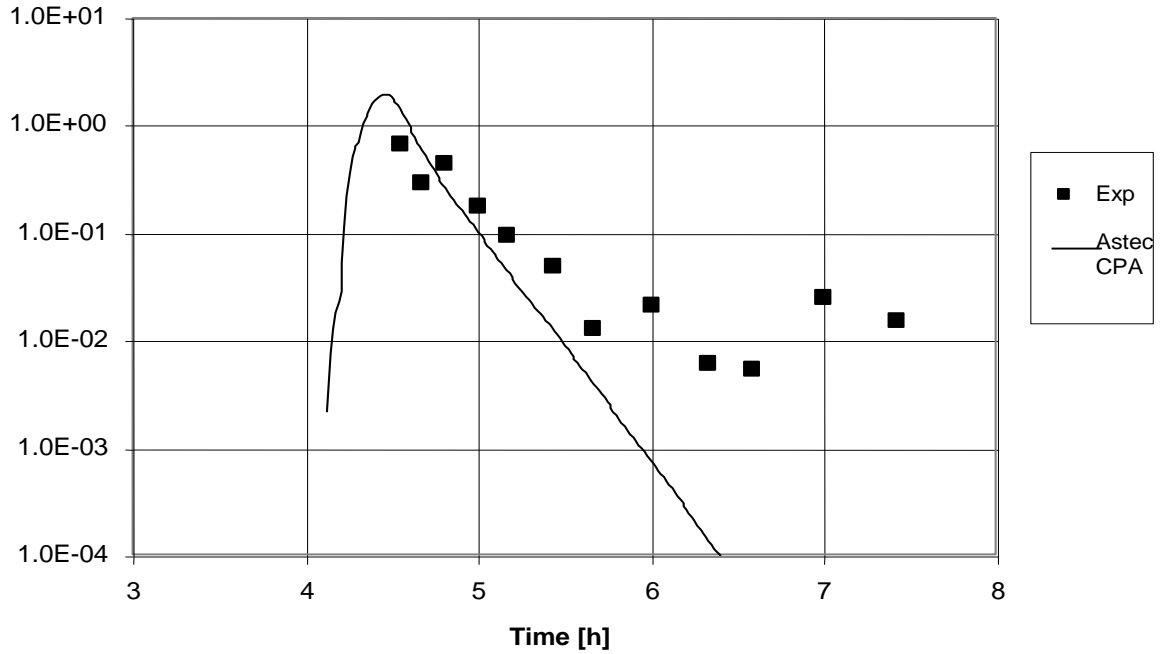


Figure 3: Comparison of measured and calculated aerosol depletion – K123 (CsI)

### K148 Total Dry Concentration (g/cm<sup>3</sup>)

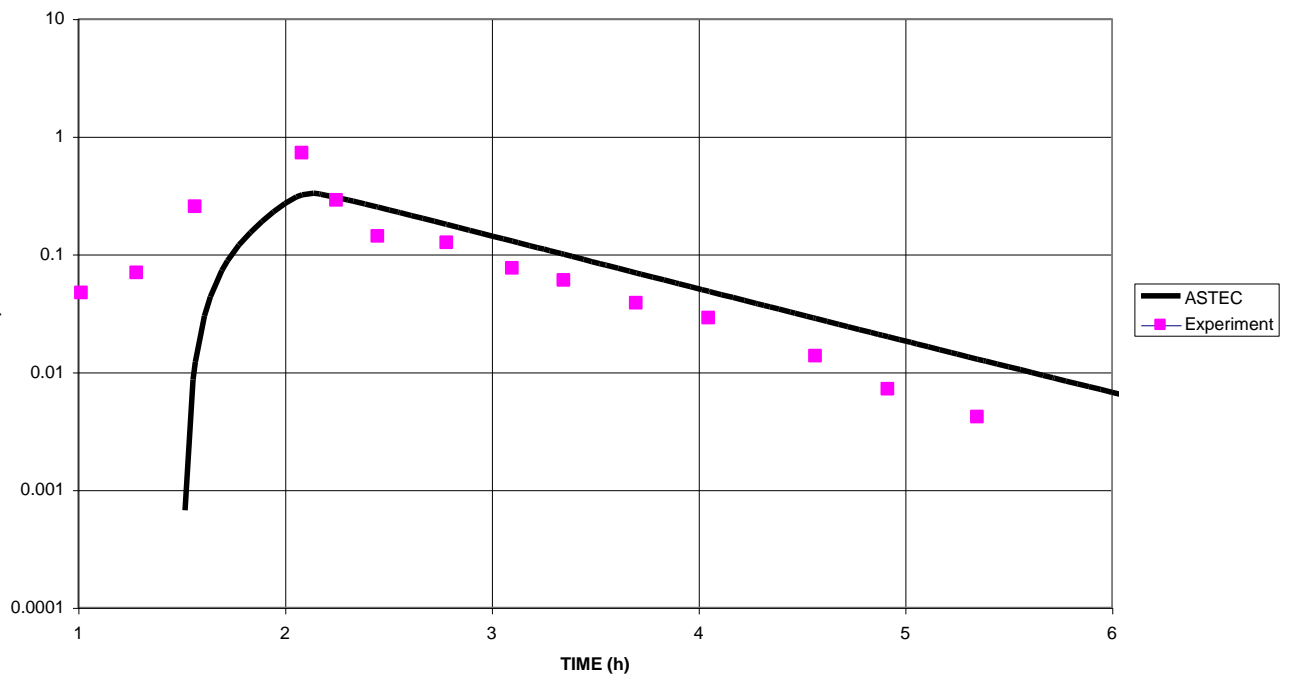


Figure 4: Comparison of measured and calculated aerosol depletion -- K148 (Ag)

### K186 Total Dry Concentration (g/cm<sup>3</sup>)

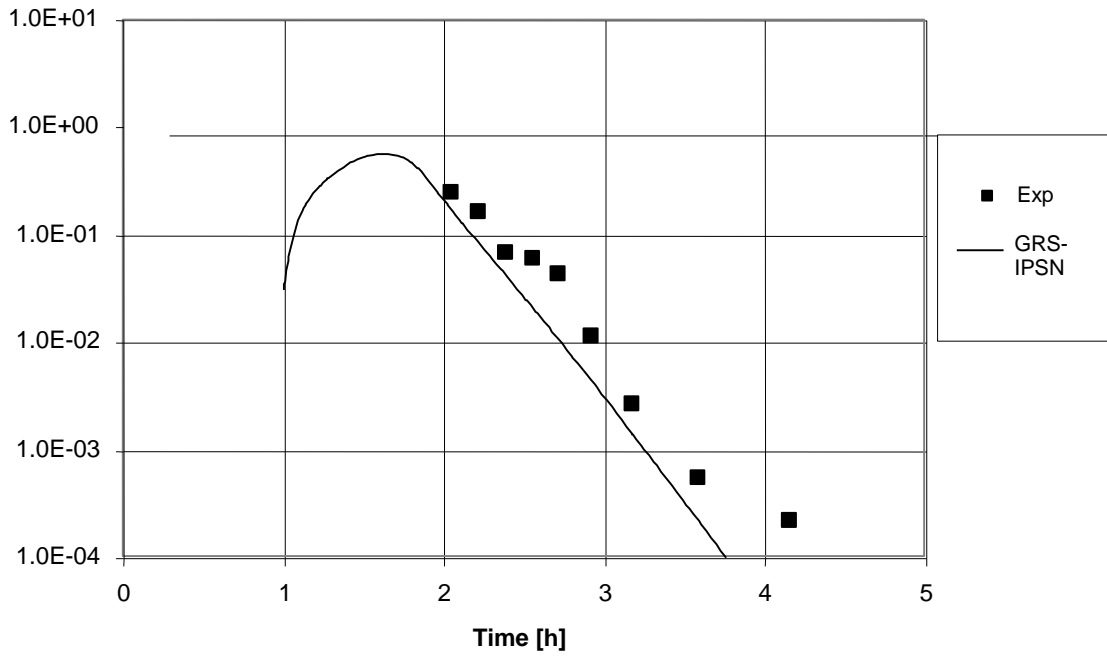


Figure 5: Comparison of measured and calculated aerosol depletion — K186 (CsOH + Ag)

### K188 Total Dry Concentration (g/cm<sup>3</sup>)

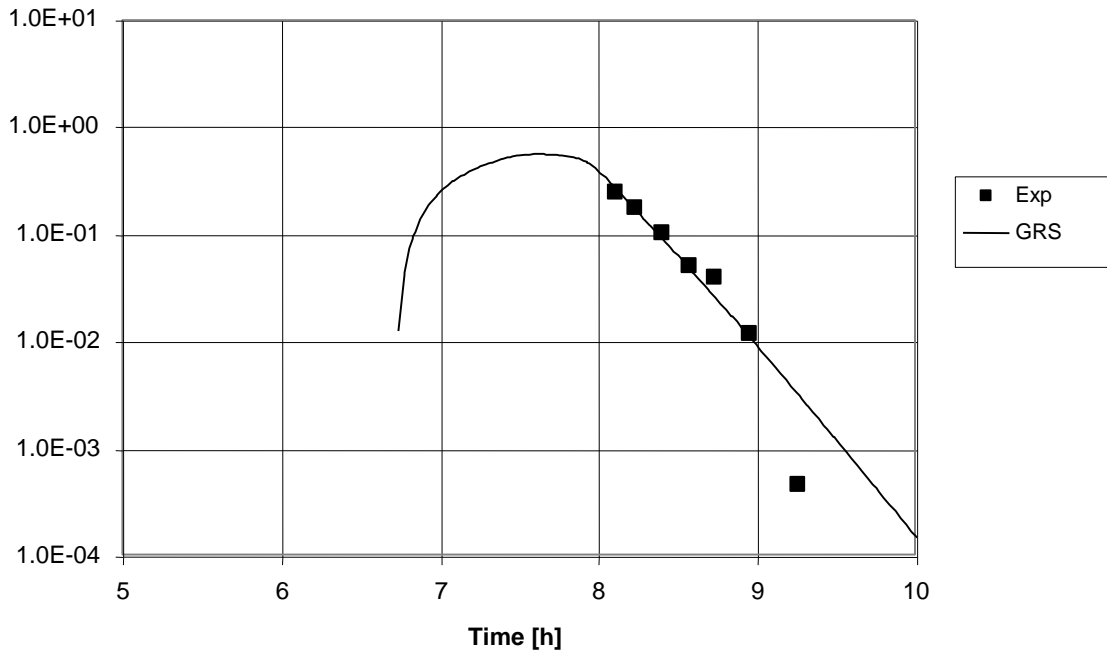
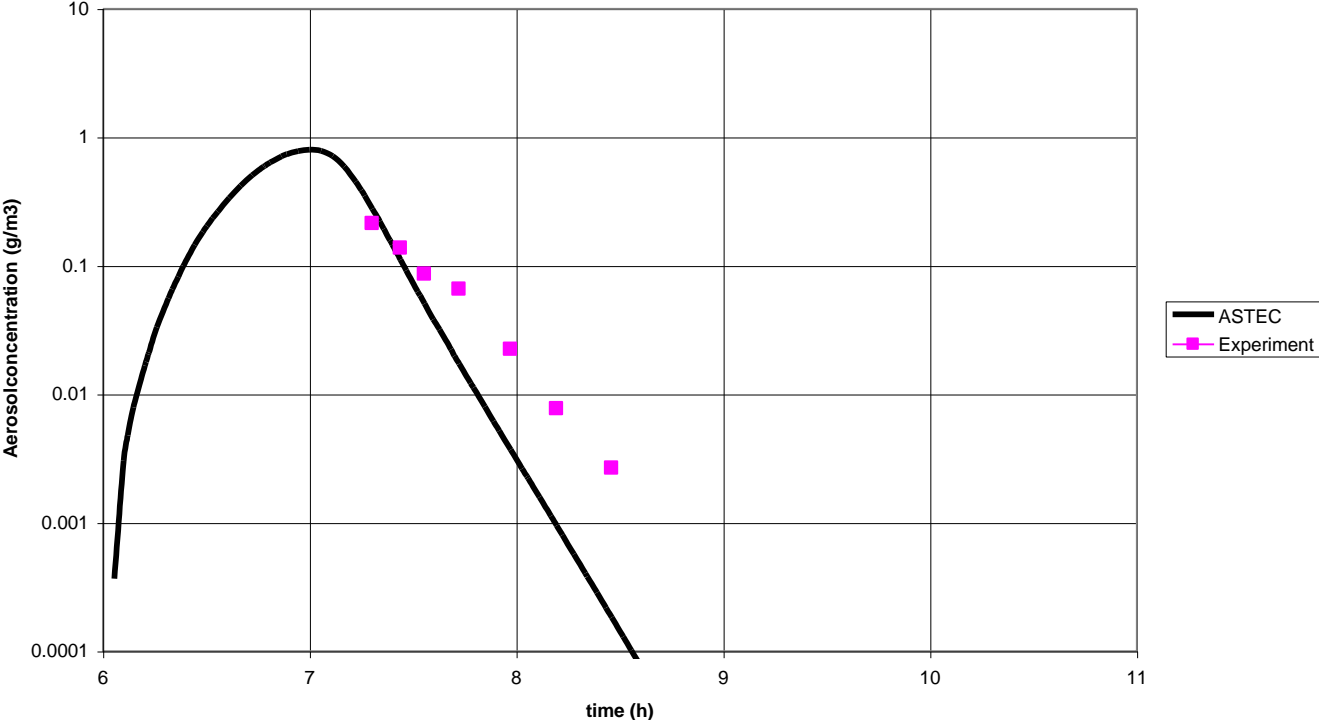


Figure 6: Comparison of measured and calculated aerosol depletion — K188 (CsOH)



**BLIND TEST K187 DRY AEROSOL CONCENTRATION (g/cm3)**



**Figure 7:** Comparison of measured and calculated aerosol depletion — blind case K187 (CSI + CsOH + Ag)